Anal. Bioanal. Electrochem., Vol. 3, No. 5, 2011, 450- 461

Analytical & Bioanalytical Electrochemistry

Full Paper

Oriented Immobilization of Anti-IgG on Amine Functionalized Carbon Nanotubes for Electrochemical Sensing of Human IgG

Alireza Lotfabadi, Hedayatollah Ghourchian*, and Susan Kaboudanian Ardestani

Institute of Biochemistry & Biophysics, University of Tehran, Enghelab Street, Tehran, Iran

*Corresponding author, Tel.: +98-21-6640 8920; Fax: +98-21-6640 4680

E-mail: hadi@ibb.ut.ac.ir (H. Ghourchian)

Received: 1 September 2011 / Accepted: 2 October 2011 / Published online: 30 October 2011

Abstract-The oriented immobilization of antibody is the most critical step in preparation of a highly sensitive immunosensor. In the present report multiwalled carbon nanotubes were treated with nitric acid followed by ethylenediamine to produce amine functionalized carbon nanotubes. To obtain a properly oriented immobilization, initially the sugar chain of antibody (anti-IgG) was oxidized to aldehyde using periodate and then the aldehyde groups were allowed to react with amine groups of carbon nanotubes. The antibody immobilization was verified using the techniques such as field emission scanning electron microscope, Fourier transform infrared, UV-Vis spectroscopy and electrochemistry. Finally determination of antigen (human IgG) was performed in the presence of conjugated horseradish peroxidase as a label, and H_2O_2 and potassium iodide as the enzyme substrates. At the optimum pH of 7.2, the detection limit of 16.6 ng/ml was obtained for determination of human IgG.

Keywords- Oriented Immobilization, Electrochemical Immunoassay, Antibody Oxidation

1. INTRODUCTION

Over the past few years, much attention has been given to promote the analytical techniques for early diagnosis of diseases [1]. Among the bio-sensing systems, a major interest has been focused on the development of immunosensors [2,3]. In the preparation of immunosensors, the oriented immobilizing of antibodies plays a major role [4]. There are some techniques to immobilize the antibodies through the Fc region. These help to leave the

Fab regions free and keep it away from the support surface. Antibody immobilization using protein A or G [5-7], site-directed biotinylation of the Fc region for immobilization on avidin or streptavidin supports [8-10] and immobilization by covalent bond through the oxidized sugar chains (Fig. 1) of antibody [11-13] on the aminated carrier are some examples of these techniques.

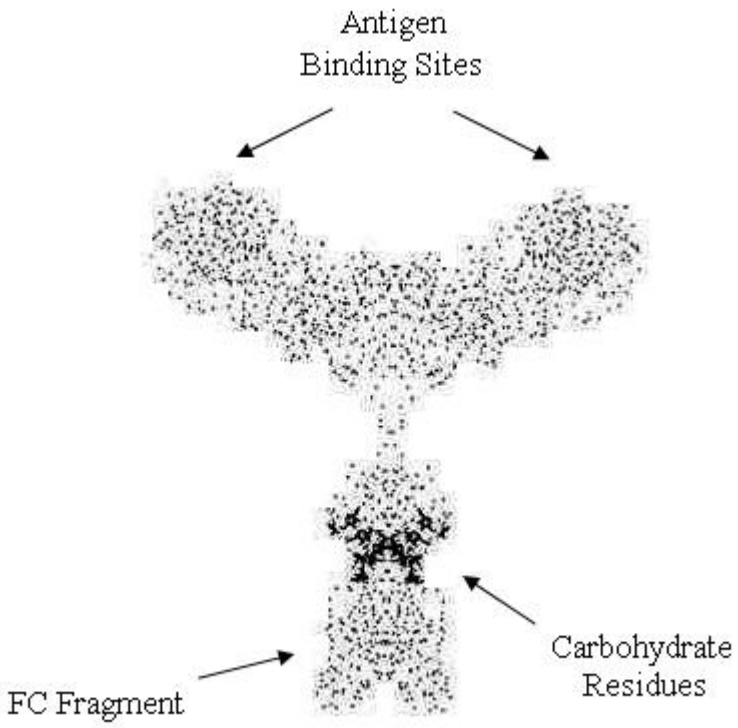

Fig. 1. Carbohydrate residues on Fc fragment of IgG. The structure was obtained from the Protein Data Bank (PDB) and visualized using Viewer Lite 5.0

Because of the unique chemical and physical properties of nanomaterials, especially large ratio of surface area to volume, they are popularly employed for many important biomedical applications. Multiwall carbon nanotubes (MWCNTs) with elite electronic, mechanical and chemical properties and their capability for functionalization have mostly been applied for modification of electrode surface [14] for biosensor applications [15-18]. High electronic conductivity of MWCNTs makes it a suitable guide to facilitate electron transfer between the electroactive species and the electrode surface.

The detection systems for immunosensors could be based on either optical, microgravimetric or electrochemical methods [2]. In case of electrochemical immunosensors, the biospecific interaction is electrochemically transformed into an electrical signal. Specifically, the interaction signal can be amplified by an enzyme which continuously generates electroactive products. Because of simple fabrication and good sensitivity, such

enzyme-amplified electrochemical immunosensors [19], have been adopted for many miniaturized and microfluidic devices. Moreover, the sandwich-type electrochemical immunosensors have gained much attention for their high specificity and sensitivity.

In the present study at first MWCNTs were amine functionalized (MWCNT-NH_2). In the other hand, carbohydrate residues of anti-human immunoglobulin G (anti-HIgG), as a typical antibody, were oxidized with periodate to produce aldehyde groups [20]. Then, the aldehyde groups on anti-IgG were allowed to react with amino groups on the surface of MWCNT-NH_2. Using a sandwich model, the horseradish peroxidase (HRP) conjugated anti-HIgG has been used as the second antibody for signal production. HRP beside hydrogen peroxides and potassium iodide (KI) as substrates was able to produce electrochemical signal for HIgG detection.

2. EXPERIMENTAL

2.1. Chemicals

Polyclonal goat anti-human immunoglobulin G (anti-HIgG) and goat anti-HIgG conjugated with HRP (anti-HIgG-HRP) were obtained from Razi Biotech Company (Kermanshah, Iran). Human tetanus immunoglobulin G (HIgG) was obtained from CSLBehring GmbH (Germany). MWCNTs, prepared by chemical vapor deposition method (purity>95 wt%, outer diameter: 8-15 nm, inner diameter: 3-5 nm, and length: ~50 μm) were provided by Timesnano Company (Chengdu, China). Bovine serum albumin (BSA), potassium dihydrogen phosphate and dipotassium hydrogen phosphate were obtained from Sigma. The other chemicals such as sodium periodate were purchased from Merck and used as delivered. A solution of 1% (w/v) BSA in 50 mM phosphate buffer solution (PBS), pH 7.2, was used as blocking buffer. Washing solution was provided by solving 0.05% (v/v) Tween-20 in PBS. Various concentrations of HIgG and anti-IgG were prepared by diluting corresponding stock solutions in the PBS. The solutions were prepared in double distilled deionized water (18 MΩ, Barnstead, Dubuque, USA) and all experiments were carried out at room temperature.

2.2. Apparatus

Fourier transform infrared (FTIR) spectra were recorded using FTIR spectrometer (Thermo Nicolet Co, USA). All Electrochemical measurements were performed using potentiostat/galvanostat (EG&G, USA). For cyclic voltammetry, a single compartment electrochemical cell (equipped with a platinum rod auxiliary electrode), an Ag/AgCl (saturated KCl) reference electrodes (both from Metrohm), and a glassy carbon (GC) disk (Φ=2 mm) shielded with Teflon as working electrode (from Azar electrode Co., Iran) were used. The sonication of electrode was carried out using ultrasonic bath (Techno-Gaz, Italy).

The morphology of modified MWCNTs was characterized using field emission scanning electron micrograph (FESEM) images, Hitachi model S-4160 (Japan) at 15 kV. The sample for FESEM analysis was obtained by dropping modified CNTs on GC electrode and evaporated in air at room temperature.

2.3. MWCNTs functionalization

MWCNTs were functionalized according to the literature [21]. Briefly, MWCNTs were dispersed in HNO_3 (35%) and sonicated in a sonication bath (30 W, 40 kHz) for 5 h. After filtration through a 0.45 μm hydrophilized PTFE membrane, a CNT pad was obtained. Finally, it was thoroughly washed with deionized water until no residual acid was detected and then dried under infrared lamp. In the next step to introduce amine groups on the surface of nano-tubs, 20 mg of thus prepared HOOC-MWCNTs was dispersed in 1 mL of $SOCl_2$ and sonicated for 5 min. The mixture was refluxed for 24 h at 50–70 ^oC, then filtered, and washed with deionized water to remove any unreacted $SOCl_2$. Then the filtrate was stirring in 5 mL of ethylenediamine for 5 days at 50–70 ^oC and filtered again. The residue was washed with anhydrous ethyl alcohol to remove any excess of ethylenediamine. The obtained NH_2-MWCNTs were dried under vacuum at room temperature. Finally, the amine functinalizations of MWCNTs was controlled using FTIR spectroscopy [22].

2.4. Oxidation of anti-HIgG

At first 1 mg/mL of anti-HIgG was incubated with 10 mM sodium periodate at 4 °C for 2 h. Then the oxidized antibody was dialyzed against phosphate buffer solution for overnight at 4 °C and immediately was used [11].

2.5. Immunosensor preparation

2 mg of MWCNT-NH_2 was suspended in 500 μL of 20 mM sodium carbonate buffer, pH 9.6. Then the oxidized anti-HIgG was immediately added to the mixture. The final concentration of anti-HIgG was adjusted to 10 mg/mL. The mixture was stirred for 2 h at room temperature. Then, to stabilize the covalent bound between anti-HIgG and MWCNT-NH_2, 50 μL of freshly prepared sodium borohydride solution (4 mg/mL) was added to the mixture and stirred occasionally over a period of 30 min at 4 °C. In order to block excess aldehyde groups of oxidized anti-HIgG, 50 μl of ethanolamine 1 M was added to the suspension. After 30 min, it was centrifuged at 7,000 rpm for 30 min at 4 °C. At the end of this process, anti-HIgG/NH_2-MWCNT was separated from supernatant and kept in refrigerator. Total concentration of the non-reacted anti-HIgG in supernatant was determined using Bradford method. Finally to prepare the immunosensor, a working GC electrode was polished carefully using 1 and 0.3 μm Al_2O_3, respectively. After that the anti-HIgG/NH_2-MWCNT were dropped on working GC electrode. Then the electrode was incubated in PBS containing 1% BSA for 1 h to block the untreated sites.

2.6. Electrochemical detection of HIgG

In order to measure the HIgG quantitatively, the immunosensor prepared in Section 2.5 (anti-HIgG/NH_2-MWCNT/GC electrode) was incubated with different concentrations of HIgG in PBS containing 1% BSA for 1 h. After washing the electrode, it was incubated with anti-HIgG-HRP (dilution 1:10000) in PBS containing 1% BSA for 1 h, followed by three times washing with washing buffer (0.05% v/v solution of Tween-20 in PBS), frequently. At such a condition and in the presence of different concentrations of HIgG the current response was recorded. The background response was also obtained in the same condition but in the absence of HIgG. The measurements were carried out in the electrochemical cell containing 2 mL PBS (50 mM, pH 7.2) comprising 2 mM H_2O_2 and 3 mM KI.

3. RESULTS AND DISCUSSION

3.1. FTIR studies

Fig. 2 represents FTIR spectra of pristine MWCNTs (dotted line), acid-functionalized MWCNTs (dashed line) and amine functionalized MWCNTs (solid line). The peak appeared at 1640 cm^{-1} is related to C=O bond. Two peaks at 2860 and 2930 cm^{-1} are due to the vibrations of C–H bond. Absorption band in the 3450 cm^{-1} region is due to O-H stretching bonds. The absorption band related to C-N bond can be observed at 1110 cm^{-1} (solid line) which indicates the appearance of new amine functional groups upon functionalization process.

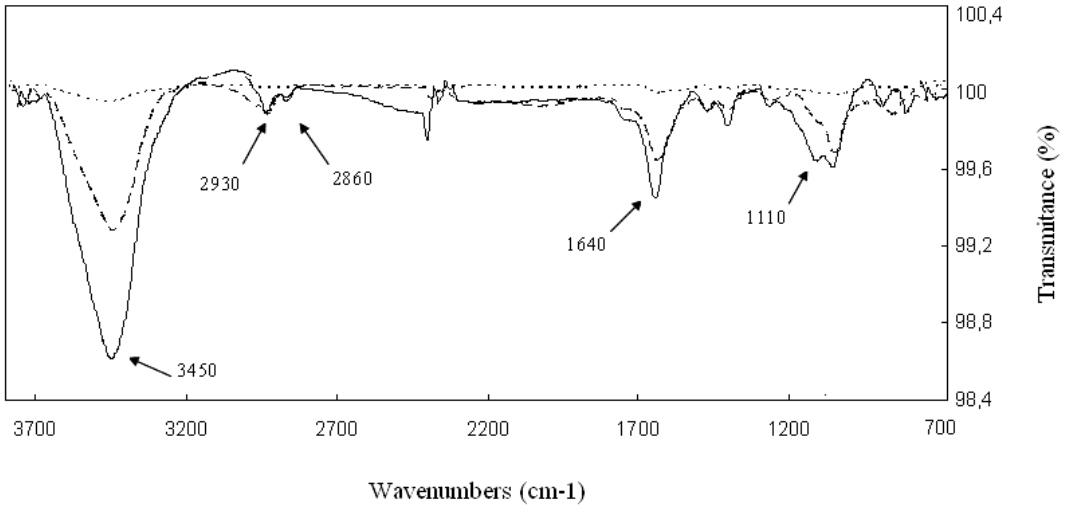

Fig. 2. FTIR spectra of pristine MWCNTs (dotted line), acid-functionalized MWCNTs (dashed line) and amine-functionalized MWCNTs (solid line)

3.2. FESEM study

The morphology of functionalized carbon nanotubes was studied using FESEM. Fig. 3a, demonstrates the amine functionalized MWCNTs absorbed on GC electrode. As seen treatment with nitric acid and sonication did not affect severely on the physical structure of MWCNTs so that they could conserve their tube-shaped structure perfectly. Fig. 3b shows the FESEM image of antibody immobilized on the MWCNTs. As seen the diameter of MWCNTs has been increased due to antibody immobilization.

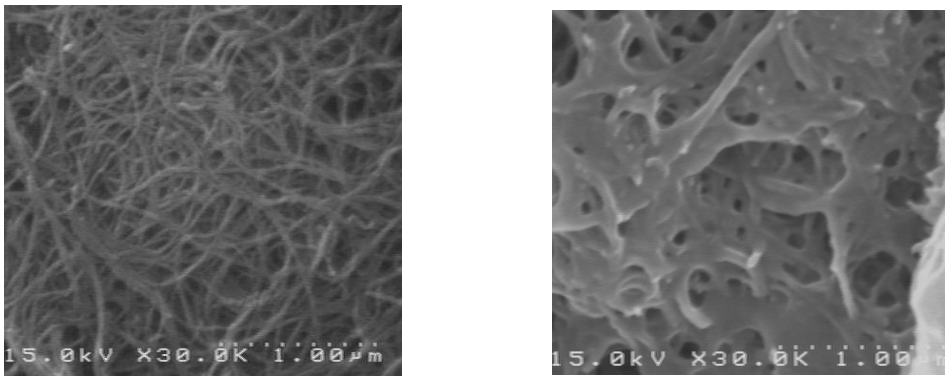

a **b**

Fig. 3. Field emission scanning electron micrograph images of (a) NH_2-MWCNTs, (b) anti-HIgG/NH_2-MWCNTs. Accelerating voltage and magnification were 15 kV and ×30000, respectively

3.3. Verification of antibody protein on NH_2-MWCNT

The antibody immobilization on NH_2-MWCNT was verified using cyclic voltammetry. The modified electrodes were placed in 2.0 mM PBS (pH 7.2) containing KNO_3 solution (1 M) and $[Fe(CN)_6]^{4-/3-}$ (2 mM). The solid line cyclic voltammogram (CV) in Fig. 4 reflects the reversible redox reaction of ferricyanide ions on bare glassy carbon (GC) electrode. Modifying the GC electrode by CNT increased the current redox peaks. This indicates an efficient improvement in the performance of GC electrode due to the high conductivity of CNTs (Fig. 4, Cycle a). By anti-HIgG loading on CNTs, the redox peak current was reduced due to decreasing the conductivity (Fig. 4, Cycle b). The peak current was further reduced after blocking the nonspecific sites with BSA (Fig. 4, Cycle c). This process was continued by addition of HIgG as antigen to the test solution (Fig. 4, Cycle d) [23,24].

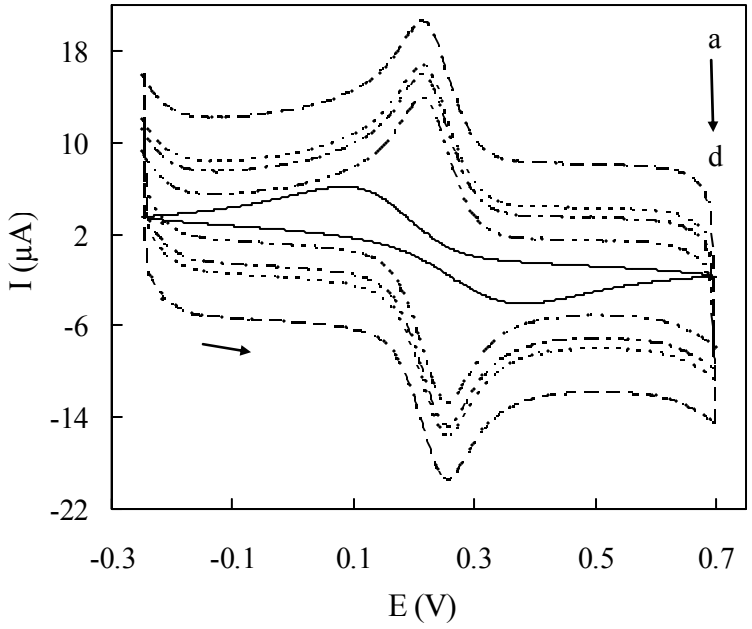

Fig. 4. CVs of $[Fe(CN)_6]^{2/3+}$ at different stages of GC electrode modification. Solid line shows the CV on GC electrode. The other CVs from outer to inner: (a) MWCNTs/GC, (b) anti-HIgG/NH_2-MWCNTs/GC,(c)(BSA)anti-HIgG/NH_2-MWCNTs/GC,(d) HIgG/(BSA)anti-HIgG/NH_2-MWCNTs/GC electrodes in 2.0 mM $[Fe(CN)_6]^{3/4-}$ and KNO_3 solution (1 M, pH 7.2). Scan rate was 50 mV s^{-1}

3.4. Cyclic voltammetry of the immunosensors in KI

Signal produced by the immunosensor (HRP-anti-HIgG/HIgG/anti-HIgG/NH_2-MWCNTs/GC electrode) was monitored using cyclic voltammetry. As shown in Fig. 5 (Cycle a), in the presence of H_2O_2 no response was observed in the potential window from 0.1 to 1 V. But by addition of KI (final concentration 3 mM) two redox couples (I-II & III-IV) were obtained at the potentials of 0.47 and 0.66 V (*vs*. Ag/AgCl) for couples I^-/I_2 (reaction 1) and I^-_3/I_2 (reaction 3), respectively (Fig. 5, Cycle b). As seen, the produced iodine may also react with iodide in bulk through reaction 2 to generate triiodide. Although, iodine is produced through reactions 1 and 3 but as shown in reaction 3, its yield is much more than that in reaction 1.

$$2I^- \leftrightarrow I_2 + 2e^- \qquad E'^0 = 0.47 \text{ V} \qquad (1)$$

$$I_2 + I^- \leftrightarrow I^-_3 \qquad (2)$$

$$2I_3^- \leftrightarrow 3I_2 + 2e^- \qquad E'^0 = 0.66 \text{ V} \qquad (3)$$

In the presence of both substrates (H_2O_2: 2 mM and KI: 3 mM) a significant increase in current response was observed at reduction potential of 0.73 V (Fig. 5, Cycle c). This is due to the catalytic effect of HRP on the production of I_2 via reactions 4 and 5:

$$HRP + H_2O_2 + I^- \rightarrow [HRP\ OI^-] + H_2O \rightarrow HRP + IO^- \quad (4)$$

$$IO^- + H^+ + I^- \rightarrow I_2 + OH^- \quad (5)$$

The produced I_2 promote reaction 2 in the forward direction. Then as expected, the anodic peak current at 0.73 V increases considerably. Due to the dependency of this current intensity to the amount of the captured HIgG, this anodic peak was selected as the redox marker for electrochemical monitoring of HIgG [25,26].

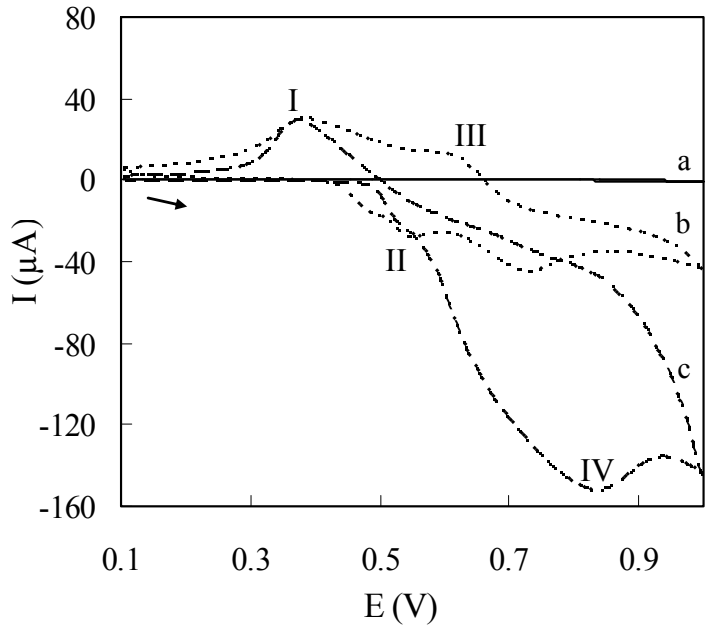

Fig. 5. CVs of the sandwich form of HRP-anti-HIgG/HIgG/anti-HIgG/NH_2-CNTs/GC electrode in: (a) H_2O_2 (2 mM), (b) KI (3 mM), (c) mixture of H_2O_2 (2 mM) and KI (3 mM). All samples prepared in 50 mM PBS (pH 7.2). Scan rate was 50 mV/s

3.5. pH optimization

To examine the pH dependency of anti-HIgG/NH_2-MWCNTs/GC electrode responses toward HIgG, the electrode was exposed to PBS buffer (0.1 M) at different pH ranging from 6.6 to 8.0. As seen in Fig. 6, the immunosensor showed a maximum current response at pH 7.2. Thus, this was selected as optimum pH for all electrochemical studies.

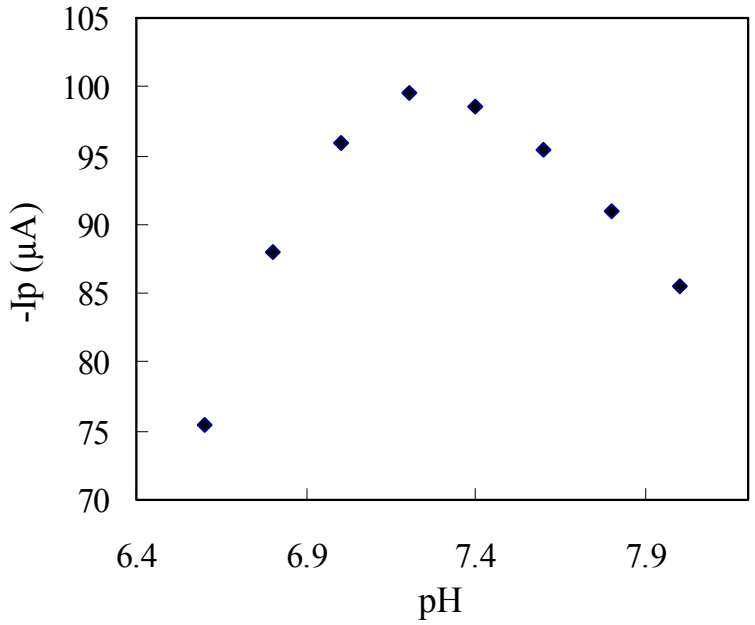

Fig. 6. pH dependency of KI anodic peak current at HRP-anti-HIgG/HIgG/anti-HIgG/NH_2-CNTs/GC electrode. The electrode was placed in 50 mM PBS buffer containing 3 mM KI and 2 mM H_2O_2, HRP-anti-HIgG and HIgG (75 ng/ml). Scan rate was 50 mV/s

3.6. Calibration curve of HIgG

For quantitative determination of HIgG, a calibration curve was plotted using I_p (the anodic peak current at 0.73 V) against antigen concentration. Fig. 7 represents the calibration plot for HIgG in the presence of H_2O_2 (2 mM) and KI (3 mM) in 0.1 M PBS, pH 7.2. With increasing the HIgG concentration in the range of 25–150 ng mL^{-1}, the anodic peak current of the redox pair of I^-_3/I_2 was increased. According to the Equation 1, and the slope obtained by Fig. 7-Inset, the detection limit of the prepared immunosensor was calculated to be 16.6 ng mL^{-1} [27]:

$$DL = ks_B/m$$

Where, S_B is standard deviation of background current and m is slope of calibration curve. Considering value of 3 for k, allows a confidence level of 99.86%.

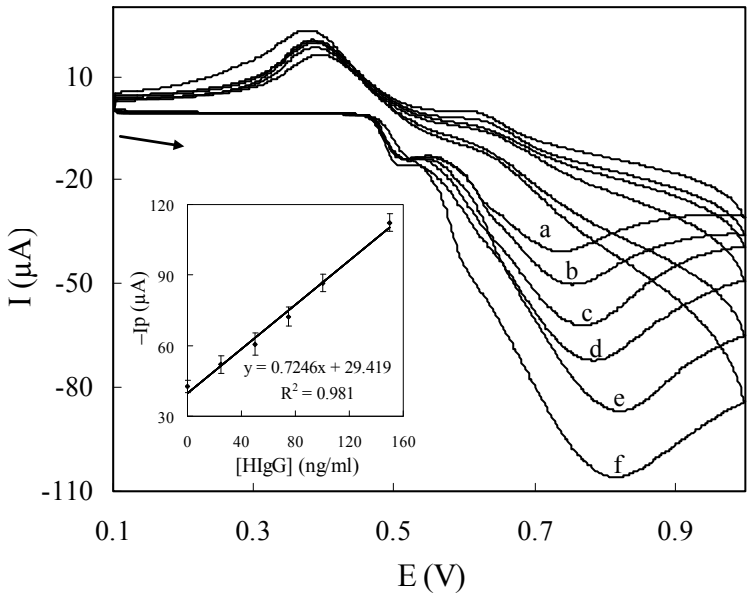

Fig. 7. CVs of the sandwich form modified electrode using different concentrations of HIgG: 0, 25, 50, 75, 100 and 150 ng/mL (from a to f), respectively. Inset shows the calibration curve for HIgG. I_p is the anodic peak current at 0.73 V. The experimental condition was the same as Fig. 6

4. CONCLUSION

Immobilization of antibodies by their oxidized sugar chain on aminated supports is a very efficient methodology to have a properly oriented immobilized antibody. In the present report a novel immunosensor was obtained using amine functionalized MWCNTs and modified anti-HIgG for electrochemical detection of human IgG. Comparing to the other techniques for oriented immobilization e.g. application of protein A, protein G or avidin-biotin system, the proposed electrochemical immunosensor seems to be faster, simpler and cheaper. Considering the importance of early diagnosis of disease and on the other hand the low detection limit of current immunosensor, this methodology seems to be applicable for biomarkers measurement at very low concentrations.

Acknowledgments

Financial supports provided by the Research Council of the University of Tehran and Pishtazteb Diognostics, Tehran, Iran are gratefully appreciated.

REFERENCES

[1] Y. Piao, Z. Jin, D. Lee, H. Lee, H. BinNa, T. Hyeon, M. KyuOh, J. Kim, and H. S. Kim, Biosens. Bioelectron. 26 (2011) 3192.
[2] B. Hock, Anal. Chim. Acta 347 (1997) 177.
[3] S. J. Kwon, E. Kim, H. Yang and J. Kwak, Analyst 131 (2006) 402.
[4] P. Batalla, M. Fuentes, V. Grazu, C. Mateo,and R. Fernandez-Lafuente, J. M. Guisan, Biomacromolecules 9 (2008) 719.
[5] J. Quinn, P. Patel, B. Fitzpatrick, B. Manning, P. Dillon, S. Daly, R. Okennedy, M. Alcocer, H. Lee, M. Morgan, and K. Lang, Biosens. Bioelectron. 14 (1999) 587.
[6] L. Bjoerck, and G. Kronvall, J. Immunol. 133 (1984) 969.
[7] E. Zacco, M. I. Pividori, and S. Alegret, Biosens. Bioelectron. 21 (2006) 1291.
[8] J. Wong, A. Chilkoti, and T. M. Vincent, Biomol. Eng. 16 (1999) 45.
[9] M. Diaz-Gonzalez, M. B. Gonzalez-Garcia, and A. Costa-Garcia, Biosens. Bioelectron. 20 (2005) 2035.
[10] W. Limbut, P. Kanatharana, B. Mattiasson, P. Asawatreratanakul, and P. Thavarungkul, Anal. Chim. Acta 561 (2006) 55.
[11] M. Fuentes, C. Mateo, J. M. Guisan, and R. Fernandez-Lafuente, Biosens. Bioelectron. 20 (2005) 1380.
[12] C. A. Wolfe, and D. S. Hage, Anal. Biochem. 231 (1995) 123.
[13] P. C. Lin, S. H. Chen, K. Y. Wang, M. L. Chen, A. K. Adak, J. R. R. Hwu, Y. J. Chen, and C. C. Lin, Anal. Chem. 81 (2009) 8774.
[14] D. Tang, and J. Ren, Electroanalysis 24 (2005) 2208.
[15] C. Lynama, N. Gilmartinb, A. I. Minetta, R. O'Kennedyb, and G. Wallacea, Carbon 47 (2009) 2337.
[16] H. Chen, and C. Lu, Chem. Mater. 20 (2008) 5756.
[17] K. Balasubramanian, and M. Burghard, Anal. Bioanal. Chem. 385 (2006) 452.
[18] B. P Lopez, and A. Merkoci, Analyst 134 (2009) 60.
[19] M. Pohanka, O. Pavlis, and P. Skladal, Sensors 7 (2007) 341.
[20] M. Lei, R. J. Hu, Y. G. Wang, Tetrahedron 62 (2006) 8928.
[21] J. S. Jeong, S. Y. Jeon, T. Y. Lee, J. H. Park, J. H. Shin, P. S. Alegaonkar, A. S. Berdinsky, and J. B. Yoo, Diamond Relat. Mater. 15 (2006) 1839.
[22] P. Rahimi, H. A. Rafiee-Pour, H. Ghourchian, P. Norouzi, and M. R. Ganjali, Biosens. Bioelectron. 25 (2010) 1301.
[23] Y. Y. Xu, C. Bian, S. Chen, and S. Xia, Anal. Chim. Acta 561 (2006) 48.
[24] L. Lu, B. Liu, C. Liu, and G. Xie, Bull. Korean Chem. Soc. 2010, Vol. 31, No. 11.
[25] W. Zhang, H. Zha, B. Yao, C. Zhang, X. Zhou, and S. Zhong, Talanta 46 (1998) 711.
[26] A. A. P. Ferreira, W. Colli, M. J. M. Alves, D. R. Oliveira, P. I. Costa, A. G. Guell, F. Sanz, A. V. Benedetti, and H. Yamanaka, Electrochim. Acta 51 (2006) 5046.

[27] D. A. Skoog, F. J. Holler, and T. A. Nieman, Principles of Instrumental Analysis, Cengage Learning, (1998).